

Suppression Limit Cycles in 2x2 Nonlinear Systems with Memory Type Nonlinearities

KARTIK CHANDRA PATRA^{1,*}, NAMRATA KAR², ASUTOSH PATNAIK³

^{1,2,3}Department of Electrical Engineering

C. V. Raman Global University, Bhubaneswar, Odisha 752054, INDIA

*Corresponding Author

*ORCID ID: 0000-0002-4693-4883

Abstract: - For several decades, the importance and weight-age of prediction of nonlinear self-sustained oscillations or Limit Cycles (LC) and their quenching by signal stabilization have been discussed, which is confined to Single Input and Single Output (SISO) systems. However, for the last five to six decades, the analysis of 2x2 Multi Input and Multi Output (MIMO) Nonlinear Systems gained importance in which a lot of literature available. In recent days' people have started discussing suppression of LC which limits the performance of most of the physical systems in the world. It is a formidable task to suppress the limit cycles for 2x2 systems with memory type nonlinearity in particular. Backlash is one of the nonlinearities commonly occurring in physical systems that limit the performance of speed and position control in robotics, automation industry and other occasions like Load Frequency Control (LFC) in multi area power systems. The feasibility of suppression of such nonlinear self-oscillations has been explored in case of the memory type nonlinearities. Backlash is a common memory type nonlinearity which is an inherent Characteristic of a Governor, used for usual load frequency control of an inter-connected power system and elsewhere. Suppression LC using pole placement technique through arbitrary selection and optimal selection of feedback Gain Matrix K with complete state controllability condition and Riccati Equation respectively and is done through state feedback. The Governing equation is $d/dt [X(t)] = (A-BK) X$: which facilitates the determination of feedback gain matrix K for close loop Poles / Eigen values placement where the limit cycles are suppressed/eliminated in the general multi variable systems. The complexity involved in implicit non-memory type or memory type nonlinearities, it is extremely difficult to formulate the problem for 2x2 systems. Under this circumstance, the harmonic linearization/harmonic balance reduces the complexity considerably. Still the analytical expressions are so complex which loses the insight into the problem particularly for memory type nonlinearity in 2x2 system and the method is made further simpler assuming a 2x2 system exhibits the LC predominately at a single frequency. Hence in the proposed work an alternative attempt has been made to develop a graphical method for the prediction of Limit Cycling Oscillations in 2x2 memory type Nonlinear systems which not only reduces the complexity of formulations but also facilitates clear insight into the problem and its solution.

The present techniques are well illustrated with an example and validated / substantiated by digital simulation (developed program using MATLAB codes) and use of SIMULINK Tool Box of MATLAB software.

The present work has the brighter future scope of:

Adapting the Techniques like Signal Stabilization and Suppression LC for 3x3 or higher dimensional nonlinear systems through an exhaustive analysis.

Analytical/Mathematical methods may also be developed for signal stabilization using both deterministic and random signals based on Dual Input Describing function (DIDF) and Random Input Describing Function (RIDF) respectively.

The phenomena of Synchronization and De-synchronization can be observed/identified analytically using Incremental Input Describing Function (IDF), which can also be validated by digital simulations.

Key-Words: - Limit Cycles, Describing function, 2x2 non-linear systems, Pole placement technique, Suppression limit cycle, Memory type nonlinearity

Received: March 17, 2024. Revised: September 4, 2024. Accepted: September 27, 2024. Published: November 19, 2024.

1 Introduction

The exhibition of limit cycle in two dimensional multi-variable non-linear systems in interconnected power systems [1] which can fit the structure [2] of a general two dimensional nonlinear systems has been addressed in the present work [3].

For the last five decades, analysis of 2 x 2 nonlinear multivariable systems gained importance specifically for the investigation of limit cycles and a good number of literature available addressing this area of research, [1], [2], [3], [4], [5], [6], [9], [10], [11], [12], [13], [14], [15], [16], [17], [18], [19], [20], [21], [22], [23], [24], [25], [26], [27], [28], [29], [30], [31], [32], [33], [34], [35], [36], [37], [38], [39], [40], [41], [42], [43], [44], [45], [46].

Existing practice of power system, interconnected with various areas through tie-lines, sometimes suffers from mismatches in frequency because of area load change and also some other abnormal conditions. The popular, simple, easy realization, low cost, robust and decentralized nature of the control strategy, the load frequency control (LFC) is used immensely. The LFC also shows poor performance for backlash nonlinearities present in the governors [4]. It has been stressed on the LFC scheme in the zone of operation avoiding the existence of limit cycle or reducing the amplitude of sustaining oscillations. It may not be always possible to have such safer zone of operation, i.e., either absence of limit cycle or reduction in amplitude of self-sustained oscillations

In the literature [5], the limit cycle induced by backlash nonlinearity is discussed and cited about the suppression of limit cycle using state feedback, but detailed analysis, well established conclusions and straight forward techniques are still lacking [6] and also confined to a single input and single output systems.

The recent literature depicts some instances of multidisciplinary applications where limit cycle oscillations have been discussed. The researchers, [47], discussed three possible scenarios, namely, stable, limit cycles and chaos arise naturally in the flow and thermal dynamics of the device. The authors, [48], formulated/initialized the cell model to the limit cycle, running one-dimensional (OD) simulations of 500 stimuli at a BCL of 300ms. In [49], the dynamic behaviour of the nonlinear system switches between a stable equilibrium point and a stable limit cycle has been discussed. In [50], the stable limit cycle has been observed in autocatalytic systems through the characteristics of the Hopf

bifurcation. In [51], the exhibition of limit cycling oscillations has been observed in Biological Oscillators having both positive and negative feedbacks. The authors, [52], have observed in natural systems a closed loop as in a stable limit cycle through reviewing empirical dynamic modelling.

Therefore, it is suggested to adopt a novel method of suppression / elimination of limit cycles using pole placement technique through state feedback. The pole placement is done (a) by arbitrary selection of poles satisfying the state controllability conditions [7], (b) by optimal selection of feedback gain matrix K using Riccati equation [8]. The problem and the solution may be addressed in the following sequels.

2 Dynamic model of the interconnected power system:

The dynamics of general 2x2 nonlinear systems representing a interconnected power system shown in Fig.1, Fig.2 & Fig.3.

The proposed paper presents the dynamics of general 2 X 2 nonlinear systems shown in Fig.1, Fig.2, Fig.3 [2], [9], [10] which uses the state variables.

The governing equation under limit cycling condition (autonomous system i.e. $u = 0$) in frequency response form is $X = -HC$ and $C = GN(X)$ leading to $X = -HGN(X)$ $X = AX$, where $A = -HGN(X)$ [2], [9] which facilitates the determination of Eigen values of the multivariable systems (illustrated in 4.1).

$$\text{Where, } X = \begin{bmatrix} X_1 \\ X_2 \end{bmatrix}, H = \begin{bmatrix} 1 & 1 \\ -1 & 1 \end{bmatrix}, C = \begin{bmatrix} C_1 \\ C_2 \end{bmatrix},$$

$$G(\omega) = \begin{bmatrix} G_1(\omega) & 0 \\ 0 & G_2(\omega) \end{bmatrix}$$

$$N(X, \omega) = \begin{bmatrix} N_1(X_1, \omega) & 0 \\ 0 & N_2(X_2, \omega) \end{bmatrix}$$

X_1, X_2 and C_1, C_2 are Amplitudes of respective Sinusoids. G_1, G_2 are magnitudes of respective transfer functions. For memory type nonlinearities $N(X)$ is replaced by their describing functions $N(X, \omega)$ [11].

It may be noted that for frequency response: input is sinusoidal and output is steady state considered, so that s (Laplace Operator) is replaced by $j\omega$.

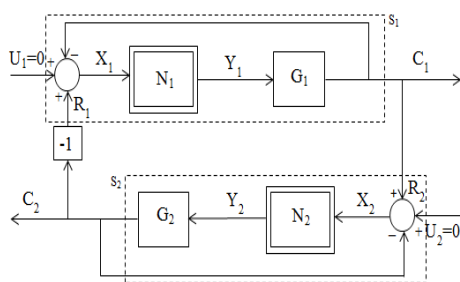


Fig. 1: A class of 2x2 nonlinear system

determination of feedback gain matrix K for closed loop poles / Eigen values placement where the limit cycles are suppressed / eliminated (illustrated in 4.1.1 and 4.1.2):

$$\text{where, } A = - \begin{bmatrix} N_1 G_1 & N_2 G_2 \\ -N_1 G_1 & N_2 G_2 \end{bmatrix} = \begin{bmatrix} -N_1 G_1 & -N_2 G_2 \\ N_1 G_1 & -N_2 G_2 \end{bmatrix},$$

$$B = \begin{bmatrix} 0 \\ 1 \end{bmatrix}$$

For memory type nonlinearity, N(X) is replaced by N(X, ω) [11].

The procedure for suppression of limit cycles in the system has been illustrated lucidly through an example. In section 3 the existence of limit cycle in systems are predicted using graphical method and substantiated by developing a digital simulation and also that with the use of SIMULINK tool box. Investigation of suppression of limit cycle in such systems has been presented in subsequent sections.

3 Prediction of limit cycles for 2x2 backlash type nonlinear system based on harmonic balance in graphical method

In general, when a closed loop system exhibits self-sustained oscillations (limit cycles), the signal at any point of the loop is transmitted around the loop to that point with no change in amplitude and phase. In other words, a system exhibits a limit cycle when the loop gain is unity and the loop phase shift is $\pm 2n\pi$ [12], where n is an integer.

For the memory type nonlinearity, there is a phase difference between input and output of the nonlinear element. This phase difference is a function of frequency of the input. The nonlinearity present in the system adds additional phase angle to the system phase angle. While predicting limit cycles exhibited by the system through graphical method, the additional phase angle contributed by the nonlinear element is to be accounted for [11].

3.1 Graphical method

The graphical method based on normalized phase diagram [11], is used for prediction of limit cycle in the system which has been lustrated through the example.

The whole system is assumed to exhibit self-oscillations predominately at a single frequency.

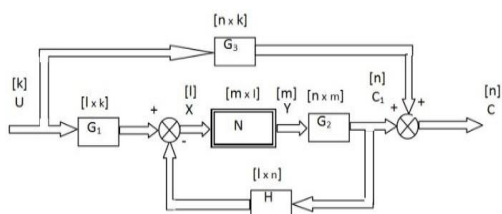


Fig. 2: Block diagram representation of a most general nonlinear multivariable system

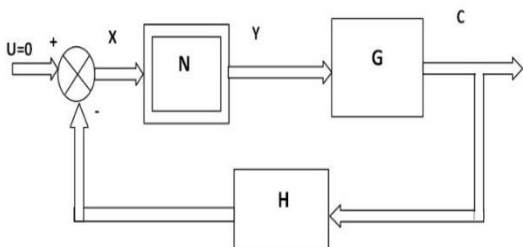


Fig. 3: Equivalent of the system of Fig. 2 with input U=0

2.1 The system dynamics of general 2 X 2 by nonlinear system with state feedback

The system dynamics with state feedback is presented in Fig.4.

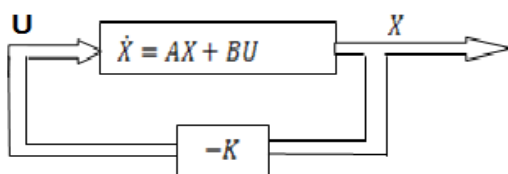


Fig. 4: A system with state feedback

The governing equation with state feedback is $d/dt[x(t)] = (A-BK) X$: which facilitates the

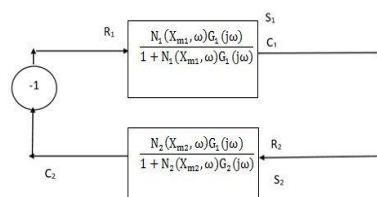


Fig. 5: Linearized equivalent for the system of Fig.1 Consider a system as shown in Fig.1 where N1 and N2 are two nonlinear elements with backlash type input-output characteristics. G1 and G2 are the transfer functions of the linear elements. Backlash nonlinearities contribute additional phase angle to the loop phase angles of G1 (j ω) and G2 (j ω) of the subsystems (s₁) and (s₂).

Replacing the nonlinear elements by their respective Describing Functions, the system of Fig. 1 can be represented as shown in Fig. 5.

“The describing function method allows us to apply familiar frequency domain techniques, used in the linear system analysis to the analysis of a class of nonlinear dynamical systems. The method can be used to predict limit cycles in nonlinear systems. The describing function method can be viewed as a “harmonic linearization” of a nonlinear element. The method provides “linear approximation” to the nonlinear element based on the assumption that the input to the nonlinear element is a sinusoid of known, constant amplitude. The fundamental harmonics of the element’s output is compared with the input sinusoid to determine the steady-state amplitude and phase relation. This relation is the describing function for the nonlinear element.

The nonlinear element is then approximately modelled by the describing function

$$N(X) = \frac{Y_1}{X} \angle \phi_1 = \frac{\text{Fundamental Component of Output}}{\text{Input}}$$

Where Y₁ = Amplitude of Fundamental Component of Output and X = Amplitude of the input sinusoid [14]

The system considered in the present work contain low pass plant transfer function and since low pass filtering of any periodic signal tends to make it sinusoidal, periodic signals within the system might be expected to be approximately sinusoidal at the nonlinearity input [15]. For the system possessing low-pass loop characteristics, the describing function (D F) analysis provides results of acceptable accuracies [10].

For the proposed work the complexity involved in the structure having the memory type nonlinearities, it would be extremely difficult to formulate and simplify the expressions in the harmonic balance method [10].

It is felt necessary to develop a graphical technique using harmonic balance method and discussed in the following lines [11].

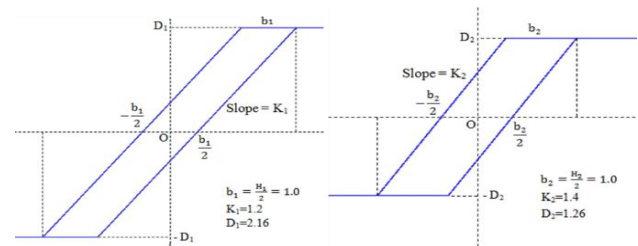
The describing function for backlash nonlinearities, shown in Fig.5, is expressed as: $N(X_m, \omega) = \frac{Y}{X_m} \angle \phi$

or

$$N(X_m, \omega) = \frac{K X_m \sqrt{\left(\frac{\pi}{2} + \beta + \frac{1}{2} \sin 2\beta\right)^2 + \cos^4 \beta}}{X_m} \angle -\tan^{-1}\left(\frac{\cos^2 \beta}{\frac{\pi}{2} + \beta + \frac{1}{2} \sin 2\beta}\right)$$

When the system exhibits limit cycle the phase diagram can be drawn as in Fig. 6(a) and subsequently the normalized phase diagram with respect to R₁ is shown as in Fig. 6(b). The determination of different quantities through graphical procedure is illustrated through example [11].

Example : where the Linear elements $G_i(s) = \frac{2}{s(s+1)^2}$ and



$G_2(s) = \frac{1}{s(s+4)}$ and the two nonlinear elements having backlash characteristics with $b_1 = b_2 = 1.0$ as shown in Fig. 5.

Fig. 6: (a) Input-output characteristics of non-linear element N₁ and (b) Input-output characteristics of non-linear element N₂

Solution: Describing function of the above Backlash Nonlinearities is expressed as

$$N(X_m, \omega) = \left| \frac{Y}{X_m} \right| \angle \phi \tag{1}$$

$$(X_m, \omega) = \frac{K X_m \sqrt{\left(\frac{\pi}{2} + \beta + \frac{1}{2} \sin \beta\right)^2 + \cos^4 \beta}}{X_m}$$

$$\angle -\tan^{-1}\left(\frac{\cos^2 \beta}{\frac{\pi}{2} + \beta + \frac{1}{2} \sin 2\beta}\right)$$

$$N(X_m, \omega) = \frac{K \sqrt{\left(\frac{\pi}{2} + \beta + \frac{1}{2} \sin \beta\right)^2 + \cos^4 \beta}}{X_m}$$

$$\angle -\tan^{-1}\left(\frac{\cos^2 \beta}{\frac{\pi}{2} + \beta + \frac{1}{2} \sin 2\beta}\right)$$

for $X_m > b/2$

$$= 0 \text{ for } X_m < b/2 \quad (2)$$

and

$$N_1(X_{m1}, \omega) = \frac{K_1}{\pi} \sqrt{\left(\frac{\pi}{2} + \beta_1 + \frac{1}{2} \sin 2\beta_1\right)^2 + \cos^4 \beta_1} \quad (3)$$

Again,

$$N_2(X_{m2}, \omega) = \frac{K_2}{\pi} \sqrt{\left(\frac{\pi}{2} + \beta_2 + \frac{1}{2} \sin 2\beta_2\right)^2 + \cos^4 \beta_2} \quad (4)$$

For subsystem (s_1):

$$\theta_{L1} = \theta_{N1}(X_{m1}, \omega) + \theta_{G1}(j\omega) \quad (5)$$

$$\theta_{L1} = \left[-\tan^{-1} \left(\frac{\cos^2 \beta_1}{\frac{\pi}{2} + \beta_1 + \frac{1}{2} \sin 2\beta_1} \right) - \frac{\pi}{2} - 2 \tan^{-1} \omega \right] \quad (6)$$

where, $\beta_1 = \sin^{-1} \left(1 - \frac{b_1}{X_{m1}} \right)$

Similarly, for subsystem (s_2):

$$\theta_{L2} = \theta_{N2}(X_{m2}, \omega) + \theta_{G2}(j\omega) \quad (7)$$

$$\theta_{L2} = \left[-\tan^{-1} \left(\frac{\cos^2 \beta_2}{\frac{\pi}{2} + \beta_2 + \frac{1}{2} \sin 2\beta_2} \right) - \frac{\pi}{2} - \tan^{-1} \frac{\omega}{4} \right] \quad (8)$$

Where,

$$\beta_2 = \sin^{-1} \left(1 - \frac{b_2}{X_{m2}} \right)$$

However in graphical method [11], while θ_{L1} traces a

circle, θ_{L2} traces a straight line.

The limit cycle conditions of the system can be represented by the phase diagram shown in Fig. 7(a) and subsequently the normalised phase diagram in Fig. 7(b).

Radius of the above mentioned circle is

$$r = \frac{1}{2 \sin \theta_{L1}} \quad (9)$$

And centre of the circle is at:

$$\left(0.5, \frac{-1}{2 \tan \theta_{L1}} \right) \quad (10)$$

The point of intersection of the circle and the straight line is at (u_i, v_i) , which can be obtained as follows:

$$u_i = \frac{v_i}{\tan \theta_{L2}} - 1 \quad (11) \text{ and,}$$

$$v_i = \frac{3 \cot \theta_{L2} + \cot \theta_{L1}}{2 \csc^2 \theta_{L2}} \pm \frac{\sqrt{(3 \cot \theta_{L2} + \cot \theta_{L1})^2 - 8 \csc^2 \theta_{L2}}}{2 \csc^2 \theta_{L2}} \quad (12)$$

The phase diagram of the system can be obtained by using the following relationship (c f .13) shown in Fig. 7(a) and the normalised one in Fig. 7(b).

From the phase diagram Fig.7 (a),

$$R_1 = X_1 + C_1, R_2 = X_2 + C_2, R_2 = C_1, R_1 = -C_2 \quad (13)$$

$$\frac{C_1}{R_1} = \frac{C_1}{C_2} = \frac{Y_1 G_1}{Y_2 G_2} = \frac{X_{m1} N_1 G_1}{X_{m2} N_2 G_2} \quad (14)$$

$$\text{Or } \frac{C_1}{R_1} = \frac{(X_{m1} G_1) \frac{K_1}{\pi} \sqrt{\left(\frac{\pi}{2} + \beta_1 + \frac{1}{2} \sin 2\beta_1\right)^2 + \cos^4 \beta_1}}{(X_{m2} G_2) \frac{K_2}{\pi} \sqrt{\left(\frac{\pi}{2} + \beta_2 + \frac{1}{2} \sin 2\beta_2\right)^2 + \cos^4 \beta_2}} \quad (15)$$

$$\text{Or } \frac{C_1}{R_1} = \frac{(K_1 X_{m1} G_1) \sqrt{\left(\frac{\pi}{2} + \beta_1 + \frac{1}{2} \sin 2\beta_1\right)^2 + \cos^4 \beta_1}}{(K_2 X_{m2} G_2) \sqrt{\left(\frac{\pi}{2} + \beta_2 + \frac{1}{2} \sin 2\beta_2\right)^2 + \cos^4 \beta_2}} \quad (16)$$

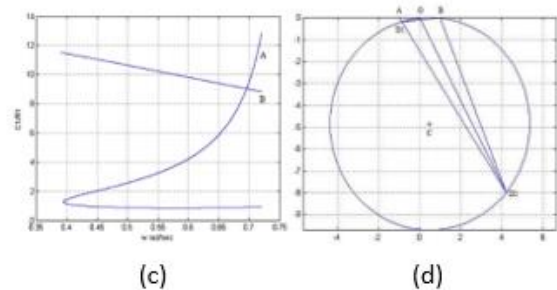
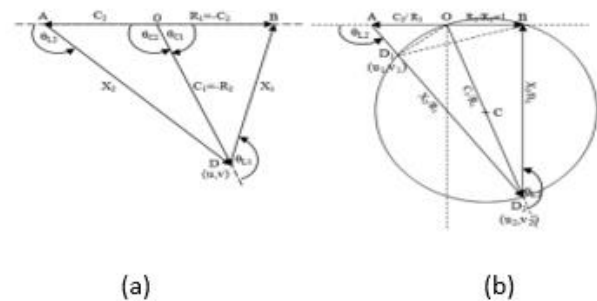


Fig. 7: (a) Phase diagram for a 2×2 nonlinear systems, (b) normalised phase diagram for a simplified generalised 2×2 nonlinear systems, (c) solution of the system, (d) normalised phase diagram for Example 1 (backlash) with $\omega = 0.6955$ radian/sec

Where, Y_1, Y_2, N_1, N_2, G_1 and G_2 are magnitude or absolute values.

From Fig. 6, $K_1 = 1.2, K_2 = 1.4$, since,

$$\left| \frac{G_1(j\omega)}{R_1} \right| = \frac{2}{\omega(\omega^2+1)}; \left| \frac{G_2(j\omega)}{R_1} \right| = \frac{2}{\omega\sqrt{16+\omega^2}}; \left| \frac{G_1}{G_2} \right| = \frac{2\sqrt{16+\omega^2}}{(\omega^2+1)}$$

Eq. (16) can be written as:

$$\frac{C_1}{R_1} = \frac{1.714 \times \sqrt{16+\omega^2} \sqrt{(\frac{\pi}{2} + \beta_1 + 1/2 \sin 2\beta_1)^2 + \cos^4 \beta_1}}{X_{m2}(\omega^2+1) \sqrt{(\frac{\pi}{2} + \beta_2 + 1/2 \sin 2\beta_2)^2 + \cos^4 \beta_2}}$$

(17)

Several normalised phase diagrams are drawn to scale (c f. Table 2) utilizing the data from Table 1. The values of

$\frac{C_1}{R_1}$ for different values of ω are calculated using Eq. (17) as well as from the graphical plots (c f. Fig. 7(d)).

Fig. 7(c) shows the variation of $\frac{C_1}{R_1}$ from the phase

diagram (curve A) and from Eq. (17) (curve B) for different values of frequency ω (c f. Table 1).

The Table 2 shows the phase diagrams for the graphical method of backlash type nonlinearity for the Example.

The point of the intersection of curve (A) and curve (B) (c f Fig. 7.c) provides the value of limit cycle frequency $\omega = 0.6955$ radian/sec. Other values of interest are determined from the Fig.7. (d), and also (cf. serial number 7 of Table 2) as:

$$\frac{C_1}{R_1} = 9.0302; \frac{X_1}{R_1} = 8.6090 \text{ And } \frac{C_1}{R_1} = 1.0; \frac{X_2}{R_1} = 9.5381$$

$$\text{Thus } X_1 = X_{m1} N_1 G_1 \frac{BD}{OD} = 4.4220;$$

$$X_2 = X_{m2} N_2 G_2 \frac{AD}{OD} = 4.8965$$

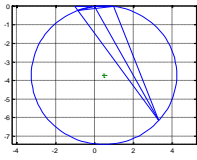
$C_1 = 4.6384$; $C_2 = 0.5136$, where X_{m1} and X_{m2} are amplitudes of sinusoids for sub system S_1 & S_2 respectively, mentioned in Table 1.

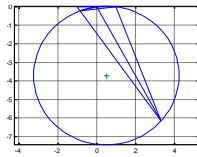
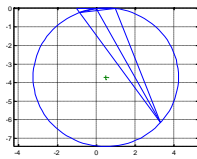
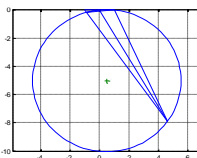
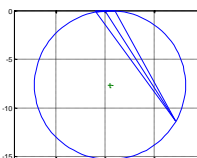
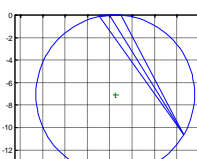
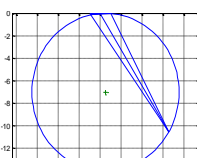
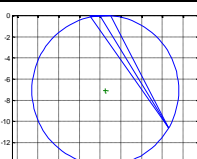
The values of X_1, X_2, C_1 & C_2 for $\omega = 0.6955$ are shown in Table.3 (c f 3.4: comparison of results).

Table-1: Values of different quantities for Example (Backlash)

ω	θ_{L1}	θ_{L2}	R (Radius)	$\frac{C_1}{R_1}$ Plot (c f Table 2)	$\frac{C_1}{R_1}$ Eq.(17)
0.600	-166.3730	-121.8119	0.508	0.8554,4.2227	9.8200
0.625	-168.6673	-122.1618	0.505	0.8616,4.9186	9.6127
0.650	-170.5142	-122.5110	0.503	0.8720,5.8676	9.4065
0.675	-172.5052	-122.8596	0.501	0.8869,7.2609	9.2017
0.700	-174.4505	-123.2074	0.500	0.9064,9.5447	8.9988
0.6961	-174.1500	-123.1532	0.500	0.9031,9.0955	9.0303
0.6955	-174.1037	-123.1448	0.551	0.9025,9.0302	9.0351 (LC)
0.72	-177.5066	-125.816	0.638	0.9084,11.500	11.87

Table-2: Phase diagrams for various values of ω and its subsequent values of r for the example using graphical method (backlash type nonlinearity)

Sl. No	ω	R- Radius	Phase diagrams	C1 / R1 from plot (cf Table 2) from eqn. 17
1	0.600	0.508		0.8554, 4.2227

2	0.625	0.505		0.8616, 4.9186
3	0.650	0.503		0.8720, 5.8676
4	0.675	0.501		0.8869, 7.2609
5	0.700	0.5003		0.9064, 9.5447
6	0.6961	0.5004		0.9031, 9.0955
7	0.6955	0.5005		0.9025, 9.0302 9.0351 X1 = 4.4220 X2 = 4.8965 C1 = 4.6384 C2 = 0.5136
8	0.7200	0.6380		0.9084, 11.500

3.2 Digital simulation for prediction of limit cycles in a 2x2 backlash type nonlinear system

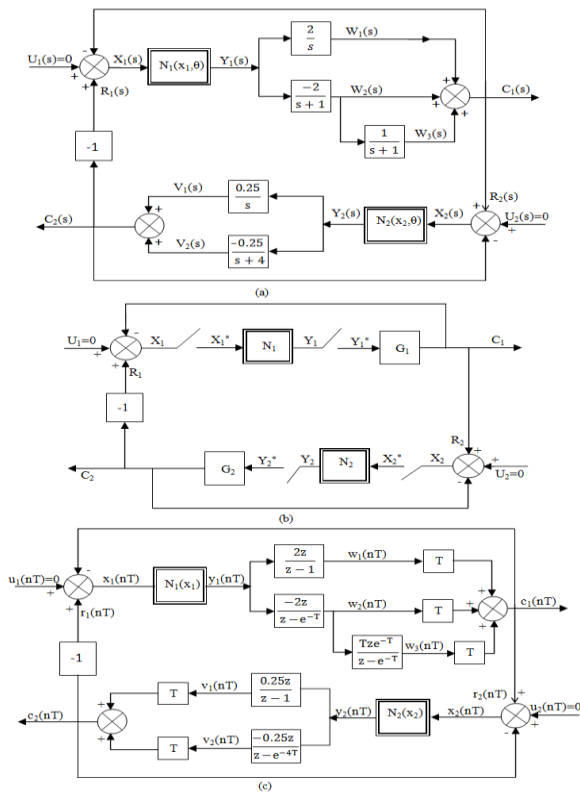


Fig.8. represents the digital simulation diagram for the example: (a) Canonical representation of the system, (b) Equivalent sample data system, (c) Digital representation in Z-domain.

Fig. 8: Digital simulation of the nonlinear system: (a) Canonical representation of the system, (b) Equivalent sample data system, (c) Digital representation in Z-domain.

The Example is revisited: $G_1(s) = \frac{2}{s(s+1)^2}$ and $G_2(s) =$

$\frac{1}{s(s+4)}$ and the nonlinear elements having backlash

characteristics with b_1 and b_2 are shown in Fig. 6(a) and 6(b).

Considering Fig-8(c),

$$y_1(nT) = f_1 x_1(nT) ; y_2(nT) = f_2 x_2(nT)$$

$$x_1(nT) = r_1(nT) - c_1(nT) ; x_2(nT) = r_2(nT) - c_2(nT)$$

In this section, following the procedure as depicted in [11], the algorithm of digital simulation has been developed to obtain the values of X_1 , X_2 , C_1 and C_2 for Backlash type nonlinearity which are then compared with those of graphical method.

For very small value of the sampling period (T):

$$TG(z) \approx G(s)$$

$$r_1(nT) = -c_2(nT) ; r_2(nT) = c_1(nT)$$

As $\frac{W_1(s)}{Y_1(s)} = \frac{2}{s}$, taking z-transform,

$$\frac{W_1(z)}{Y_1(z)} = 2 \left(\frac{z}{z-1} \right) = \frac{2}{(1-z^{-1})}$$

or

$$W_1(z) = 2Y_1(z) + z^{-1}W_1(z)$$

Taking inverse z-transform, we get,

$$w_1(nT) = 2y_1(nT) + w_1[(n-1)T]$$

Again, $\frac{W_2(s)}{Y_1(s)} = \frac{-2}{s+1}$

$$\frac{W_2(z)}{Y_1(z)} = \frac{-2z}{z-e^{-T}} = \frac{-2}{1-z^{-1}e^{-T}} \quad \text{or}$$

$$W_2(z) = -2Y_1(z) + z^{-1}e^{-T}W_2(z)$$

Taking inverse z-transform, we get,

$$w_2(nT) = -2y_1(nT) + e^{-T}w_2[(n-1)T]$$

Since, $TG(z) \approx G(s)$

$$\text{Hence, } C_1(z) = T[W_1(z) + W_2(z) + W_3(z)]$$

Applying inverse z-transform, we get,

$$c_1(nT) = T[w_1(nT) + w_2(nT) + w_3(nT)]$$

Again, $C_2(z) = T[V_1(z) + V_2(z)]$

Taking inverse z-transform,

$$c_2(nT) = T[v_1(nT) + v_2(nT)].$$

A relevant computer programme in MATLAB code using the above algorithm yields the results. The Results/Images of digital simulation along with that of using SIMULINK are shown in Fig.10 and the numerical values obtained there from are shown in Table.3 for the Example

3.3 Use of SIMULINK toolbox in MATLAB for prediction of limit cycles in 2x2 backlash type nonlinear system

In this section, the SIMULINK toolbox of MATLAB is used and accordingly the values of X_1 , X_2 , C_1 and C_2 for backlash type nonlinearities are obtained and compared with those of graphical method, and digital simulation.

The Example is re visited:

Fig.9 shows the SIMULINK representation for prediction of Limit Cycles and Fig. 10 shows the Results /Images of the Example (Back lash), obtained from Digital Simulation, developed here and also that with use of SIMULINK Tool Box.

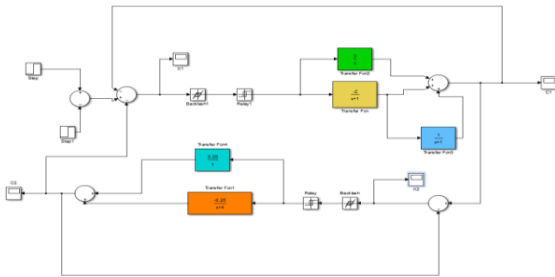


Fig. 9: SIMULINK representation for prediction of limit cycle of the Example

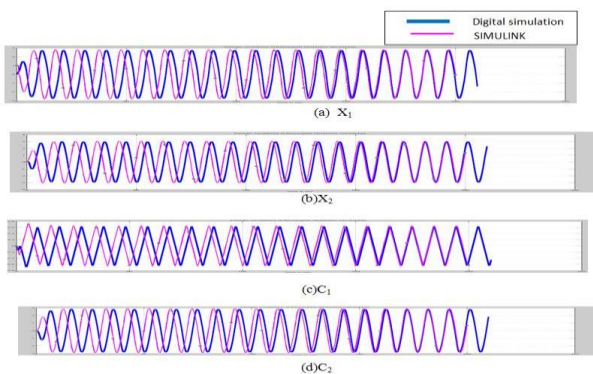


Fig. 10: Comparison of Results/Images by Digital Simulation and also that with use of SIMULINK tool box for the Example (backlash): (a) Input X_1 for S_1 , (b) Input X_2 for S_2 , (c) Output C_1 for S_1 , (d) Output C_2 for S_2

3.4 Comparison of Results

In this section, the numerical results obtained from graphical, digital simulation methods and use of SIMULINK are compared as shown in Table 3.

Table-3: Comparison of results obtained through the different methods for example (backlash).

Methods of Computation	ω	X_1	X_2	C_1	C_2
Graphical	0.6955	4.42	4.89	4.630	0.510
Digital simulation	0.7550	4.44	4.62	4.40	0.600
SIMULINK	0.7391	4.42	4.60	4.40	0.600

4 Suppression of limit cycle in 2x2 nonlinear system using pole placement technique

Limit cycles or self-sustained oscillations of a two input two output systems can be suppressed by pole placement technique. The problem of placing the closed loop poles or Eigen values of the closed loop systems at the desired location using state feedback through an appropriate state feedback gain matrix is dealt here. Necessary and sufficient condition for arbitrary pole placement is that the system be completely state controllable [7]. This can be achieved by classical as well as optimal pole placement techniques [8] and explained subsequently. The optimal pole placement has been illustrated through backlash type nonlinearity using state feedback.

4.1 Determination of Eigen values (poles) for existence of limit cycles in 2x2 nonlinear system

The most general multivariable nonlinear system [2] is shown in Fig. 2. The limit cycles may exhibit in an autonomous system (input $U=0$) where Fig. 2 can be represented in simplified form as shown in Fig. 3. Making use of the first harmonic linearization of the nonlinear elements, the matrix equation for the system of Fig.3 can be expressed as

$$X = -HC, \text{ where } C = GN(x) X. \text{ Hence,} \\ X = -HGN(x) X = AX, \quad (18) \\ \text{Where, } A = -HGN(x)$$

Realizing Eq. (18) as a transformation of the vector X onto itself, it is noted that for a limit cycle to exist the following two conditions should be satisfied [9]

- (i) For every non-trivial solution of X , the matrix A must have an Eigen value λ equal to **unity**, and

(ii) The Eigen vector of “A” corresponding to this unity Eigen value must be coincident with X.

The Example is re visited: Where the linear elements:

$G_1(s) = \frac{2}{s(s+1)^2}$ and $G_2(s) = \frac{1}{s(s+4)}$ and the two nonlinear elements having backlash characteristics with $b_1 = b_2 = 1.0$ as shown in Fig. 6.

Solution: $G = \begin{bmatrix} G_1 & 0 \\ 0 & G_2 \end{bmatrix}$; $N(x) = \begin{bmatrix} N_1(X_1) & 0 \\ 0 & N_2(X_2) \end{bmatrix}$; $H =$

$\begin{bmatrix} 1 & 1 \\ -1 & 1 \end{bmatrix}$; $X = \begin{bmatrix} X_1 \\ X_2 \end{bmatrix}$ and $C = \begin{bmatrix} C_1 \\ C_2 \end{bmatrix}$

Therefore, $A = -HGN = \begin{bmatrix} 1 & 1 \\ -1 & 1 \end{bmatrix} \begin{bmatrix} G_1 & 0 \\ 0 & G_2 \end{bmatrix} \begin{bmatrix} N_1 & 0 \\ 0 & N_2 \end{bmatrix}$

$$= - \begin{bmatrix} N_1 G_1 & N_2 G_2 \\ -N_1 G_1 & N_2 G_2 \end{bmatrix}$$

$$\text{or } A = \begin{bmatrix} -N_1 G_1 & -N_2 G_2 \\ N_1 G_1 & -N_2 G_2 \end{bmatrix}$$

The Eigen values of matrix A can be determined from the characteristic equation $|\lambda I - A| = 0$

$$\text{Whence, } \left| \begin{bmatrix} \lambda & 0 \\ 0 & \lambda \end{bmatrix} - \begin{bmatrix} -N_1 G_1 & -N_2 G_2 \\ N_1 G_1 & -N_2 G_2 \end{bmatrix} \right| = 0$$

$$\text{Or, } \left| \begin{bmatrix} \lambda + N_1 G_1 & N_2 G_2 \\ -N_1 G_1 & \lambda + N_2 G_2 \end{bmatrix} \right| = 0$$

$$\text{Or, } \lambda^2 + \lambda(N_1 G_1 + N_2 G_2) + 2N_1 N_2 G_1 G_2 = 0 \quad (19)$$

From Table 2 (Graphical analysis), frequency of oscillations $\omega = 0.6955$ radian/sec, $X_1 = 4.42$, $X_2 = 4.89$ and

N_1 & N_2 are calculated at this value of ω using Eq. (3) and Eq. (4) respectively.

Where, $\beta_1 = \sin^{-1}(1 - \frac{b_1}{X_{m1}})$ and

$$\beta_2 = \sin^{-1}(1 - \frac{b_2}{X_{m2}})$$

As mentioned in Table 1, the values of X_{m1} and X_{m2} are

2.3 and 1.4 respectively and $b_1 = b_2 = 1$,

$$\beta_1 = \sin^{-1}(1 - \frac{1}{2.3}) \text{ Or } \beta_1 = \sin^{-1}(1 - 0.4347)$$

$$\text{Or } \beta_1 = \sin^{-1}(0.5652)$$

$$\text{Or } \beta_1 = 0.6 \text{ radian} = 34.42^\circ$$

Similarly, $\beta_2 = \sin^{-1}(1 - \frac{1}{1.4})$ or

$$\beta_2 = \sin^{-1}(1 - 0.7143)$$

$$\text{Or } \beta_2 = \sin^{-1}(0.2857) = 0.289 \text{ radian} = 16.60$$

From Fig. 3, $K_1 = 1.2$ and $K_2 = 1.4$

Substituting the values of β_1 and K_1 in Eq. (3), we get,

$$N_1(X_{m1}, \omega) = \frac{1.2}{\pi} \sqrt{\left(\frac{\pi}{2} + 0.6 + \frac{1}{2} \sin 2 \times 34.42^\circ\right)^2 + \cos^4(34.42^\circ)}$$

$$\text{Or } N_1(X_{m1}, \omega) = 0.382 \times \sqrt{4.615} = 1.04 \quad (20)$$

Substituting the values of β_2 and K_2 in Eq. (4), we get,

$$N_2(X_{m2}, \omega) = \frac{1.4}{\pi} \sqrt{\left(\frac{\pi}{2} + 0.289 + \frac{1}{2} \sin 2 \times 16.60^\circ\right)^2 + \cos^4(16.60^\circ)}$$

$$\text{Or } N_2(X_{m2}, \omega) = 0.446 \times \sqrt{5.395} = 1.0359. \quad (21)$$

Calculating the values of $|G_1|$ and $|G_2|$ for $\omega = 0.6955$

(c f Table 1 and 2)

$$G_1(s) = \frac{2}{s(s+1)^2} \text{ or } G_1(j\omega) = \frac{2}{j\omega(j\omega+1)^2} \text{ or } |G_1(j\omega)| =$$

$$\frac{2}{\sqrt{(\omega-\omega^3)^2+(2\omega^2)^2}} = \frac{2}{\omega(\omega^2+1)}$$

$$|G_1(0.6955)| = \frac{2}{\sqrt{(0.6955-0.6955^3)^2+(2 \times 0.6955)^2}} = |G_1| = 1.938(22)$$

$$\text{Similarly, } G_2(s) = \frac{1}{s(s+4)} \text{ or } G_2(j\omega) = \frac{1}{j\omega(j\omega+4)} \text{ or}$$

$$|G_2(j\omega)| = \frac{1}{\sqrt{(\omega^2)^2+(4\omega)^2}}$$

$$|G_2(0.6955)| = \frac{1}{\sqrt{(0.6955^2)^2+(4 \times 0.6955)^2}}$$

$$= |G_2| = 0.354. \quad (23)$$

Substituting the values of N_1, N_2, G_1, G_2 in Eq. (19), we get

$$\lambda^2 + 2.384\lambda + 1.478 = 0$$

$$\text{Whence, } \lambda_1, \lambda_2 = -1.1917 \pm 0.2406j \quad (24)$$

At these values of Eigen values, the images of limit cycle oscillations for X_1, X_2, C_1 and C_2 are shown in Fig. 9 (digital simulation and SIMULINK).

4.1.1 Pole placement for suppression of limit cycles of the Example. (backlash)

Arbitrary pole placements may be possible if the system is completely state controllable [7].

The controllability matrix

$$S = [B \quad AB \quad A^2B \quad \dots] \neq 0 \quad (25)$$

$$\text{Where, } A = \begin{bmatrix} -N_1G_1 & -N_2G_2 \\ N_1G_1 & -N_2G_2 \end{bmatrix} \text{ and } B = \begin{bmatrix} 0 \\ 1 \end{bmatrix}$$

From Table 2 for Example 1(Graphical analysis),

$$\omega = 0.6955 \text{ radian/sec, } X_1= 4.42, X_2= 4.89.$$

The values of N_1 and N_2 are shown in Eq. (20) and Eq. (21) as 1.041 and 1.035 respectively.

And $|G_1(j\omega)|, |G_2(j\omega)|$ at 0.6955 are shown in Eq. (22) and Eq. (23) as 1.938 and 0.354 respectively.

On substitution of these values we obtain,

$$AB = \begin{bmatrix} -2.017 & -0.3664 \\ 2.017 & -0.3664 \end{bmatrix} \times \begin{bmatrix} 0 \\ 1 \end{bmatrix} = \begin{bmatrix} -0.3664 \\ -0.3664 \end{bmatrix}$$

Hence, the controllability matrix comes out to be,

$$S = \begin{bmatrix} 0 & -0.3664 \\ 1 & -0.3664 \end{bmatrix}$$

Taking its determinant, we obtain,

$$|S| = \begin{vmatrix} 0 & -0.3664 \\ 1 & -0.3664 \end{vmatrix} = 0.3664 \neq 0$$

Therefore, the system is completely state controllable and arbitrary pole placement is possible.

From state space equations, we know that:

$$\frac{d}{dt}[x(t)] = AX + Bu \quad (26)$$

The system under autonomous state is represented as shown in Fig.10

$$\text{From Fig. 10, the control law } u = -KX \quad (27)$$

Where $K = [k_1 \quad k_2]$ is the feedback matrix.

Replacing u in Eq. (26) by Eq. (27), we get,

$$\frac{d}{dt}[x(t)] = (A-BK)X \quad (28)$$

$$\text{Where, } A = \begin{bmatrix} -N_1G_1 & -N_2G_2 \\ N_1G_1 & -N_2G_2 \end{bmatrix}, B = \begin{bmatrix} 0 \\ 1 \end{bmatrix}$$

Taking $|\lambda I - (A - BK)| = 0,$

$$(\lambda^2 + \lambda(N_2G_2 + N_1G_1 + k_2) + (2N_1N_2G_1G_2 - N_2G_2k_1 + k_2N_1G_1)) = 0 \dots \dots (29)$$

On substitution of the values of N_1, N_2 (from Eq. 20 and Eq. 21 as $N_1=1.041$ & $N_2=1.035$ respectively), G_1 and G_2 are calculated as $G_1=1.938, G_2=0.354$ for $\omega = 0.6955$ radian/sec (c f Table 2) in Eq. (29), we get,

$$(\lambda^2 + \lambda(0.3664 + 2.017 + k_2) + (2 \times 0.3664 \times 2.017 - 0.3664 \times k_1 + k_2 \times 2.017)) = 0$$

Or

$$(\lambda^2 + \lambda(2.3834 + k_2) + (1.478 - 0.3664 \times k_1 + k_2 \times 2.017)) = 0$$

... .. (30)

Where k_1 and k_2 can be selected arbitrarily.

4.1.2 Optimal selection of feedback matrix K using Riccati Equation for the Example

The Riccati equation is,

$$A^T P + PA - PBR^{-1}B^T P + Q = 0 \text{ and } K = R^{-1}B^T P$$

Assuming $R=1, B=\begin{bmatrix} 0 \\ 1 \end{bmatrix}$ and $Q = \begin{bmatrix} 1 & 0 \\ 0 & 0 \end{bmatrix}$ we calculate the matrix "P".

Let $P = \begin{bmatrix} p_1 & p_2 \\ p_2 & p_4 \end{bmatrix}$ therefore,

$$A^T P = \begin{bmatrix} -N_1G_1 & N_1G_1 \\ -N_2G_2 & -N_2G_2 \end{bmatrix} \begin{bmatrix} p_1 & p_2 \\ p_2 & p_4 \end{bmatrix} = \begin{bmatrix} -N_1G_1p_1 + N_1G_1p_2 & -N_1G_1p_2 + N_1G_1p_4 \\ -N_2G_2p_1 - N_2G_2p_2 & -N_2G_2p_2 - N_2G_2p_4 \end{bmatrix} \dots (31a)$$

$$PA = \begin{bmatrix} p_1 & p_2 \\ p_2 & p_4 \end{bmatrix} \begin{bmatrix} -N_1G_1 & -N_2G_2 \\ N_1G_1 & -N_2G_2 \end{bmatrix} = \begin{bmatrix} -N_1G_1p_1 + N_1G_1p_2 & -N_2G_2p_1 - N_2G_2p_2 \\ -N_1G_1p_2 + N_1G_1p_4 & -N_2G_2p_2 - N_2G_2p_4 \end{bmatrix} (31b)$$

$$PBR^{-1}B^T P = \begin{bmatrix} p_1 & p_2 \\ p_2 & p_4 \end{bmatrix} \begin{bmatrix} 0 \\ 1 \end{bmatrix} \begin{bmatrix} 0 & 1 \end{bmatrix} \begin{bmatrix} p_1 & p_2 \\ p_2 & p_4 \end{bmatrix} = \begin{bmatrix} p_2^2 & (p_2 p_4) \\ (p_2 p_4) & p_4^2 \end{bmatrix} (31c)$$

$$Q = \begin{bmatrix} 1 & 0 \\ 0 & 0 \end{bmatrix} (31d)$$

Adding Eqn. (31a), (31b), (31d) and subtracting Eq. (31c) and substituting the values of N_1, G_1, N_2 and G_2 we get,

$$\begin{bmatrix} -2.89p_1 + 2.89p_2 - p_2^2 + 1 & -2.182p_2 + 1.445p_4 - 0.7366p_1 - p_2p_4 \\ -2.182p_2 + 1.445p_4 - 0.7366p_1 - p_2p_4 & -1.47p_2 - p_4^2 \end{bmatrix}$$

Whence, $-1.47p_2 - p_4^2 = 0$

$$p_2 = \frac{-p_4^2}{1.47} (32a)$$

$$-2.89p_1 + 2.89p_2 - p_2^2 + 1 = 0$$

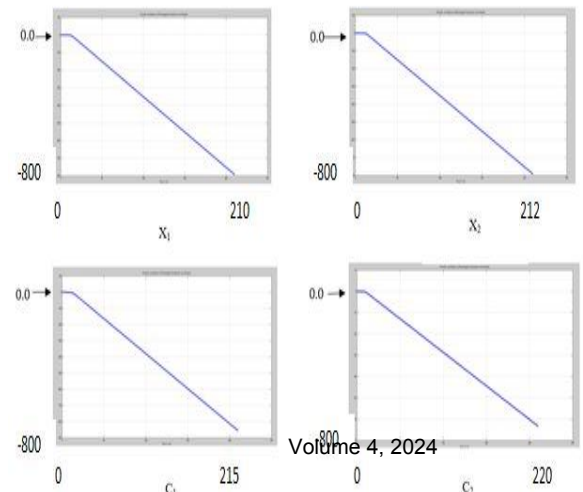
$$p_1 = p_2(1 - 0.346p_2) - 0.346$$

$$-2.182p_2 + 1.445p_4 - 0.7366p_1 - p_2p_4 = 0 (32b)$$

Substituting Eq. (32a) in Eq. (32b), we get,

$$0.1178p_4^4 + 0.68p_4^3 + 1.984p_4^2 + 1.563p_4 - 0.255 = 0 (32c)$$

Solving the above polynomial from Eq. (32c) we will get four roots,



Roots of the above polynomial,

$$(p_4)_1 = 0.1378 \text{ (real)}$$

$$(p_4)_2 = 1.375 \angle 180^\circ$$

$$(p_4)_3 = 3.379 \angle 132.146^\circ$$

$$(p_4)_4 = 3.379 \angle -132.146^\circ$$

Considering only the first real root $(P_4)_1$ as P_4 , we will find out the other elements of matrix "P".

$$p_2 = \frac{-p_4^2}{1.47}$$

$$p_2 = -0.0129$$

$$p_1 = p_2(1 - 0.346p_2) - 0.346$$

$$p_1 = -0.3589$$

$$\text{Hence, } P = \begin{bmatrix} -0.3589 & -0.0129 \\ -0.0129 & 0.1378 \end{bmatrix}$$

$$\text{Feedback matrix } K = R^{-1}B^T P =$$

$$[0 \ 1] \begin{bmatrix} -0.3589 & -0.0129 \\ -0.0129 & 0.1378 \end{bmatrix} = [-0.0192 \ 0.0187] =$$

$$[k_1 \ k_2] \quad (32d)$$

Substituting values of k_1 and k_2 in Eq. (30), yields,

$$\lambda^2 + 2.402\lambda + 1.5223 = 0 \quad (33)$$

The roots of Eq. (33) are:

$$\lambda_1, \lambda_2 = -1.2010 \pm j0.2833$$

The comparison of Eigen values/poles, feedback constants with system conditions are shown in Table. 4.

Table-4: Poles/Eigen values of the system in the presence and absence of limit cycles for the example.

System Condition	Roots	State feedback constants
Limit cycle exhibits	$\lambda = -1.917 \pm j0.240$	$k_1 = 0, k_2 = 0$
Limit cycle does not exist (Optimal selection of gain K)	$\lambda = -1.201 \pm j0.2833$	$k_1 = -0.0192, k_2 = 0.0187$

Fig.11 Shows the Results/Images for pole placement of the Example (backlash) by optimal selection of state feedback gain K.

Fig. 11: Results/images for Pole placement of (a)input X_1 for S_1 , (b) input X_2 for S_2 , (c) output C_1 for S_1 and (d)output C_2 for S_2 from Example 1 (backlash) for poles

placed at $\lambda_1, \lambda_2 = -1.2010 \pm j0.2833$

($K = [-0.0192 \ 0.0187] = [k_1 \ k_2]$ using Riccati Equation)

4.1 Determination of Eigen values (poles) for existence of limit cycles in 2x2 nonlinear system

From Fig.3 and Eq. (18)

$$A = -HGN \quad \text{Where } H = \begin{bmatrix} 1 & 1 \\ -1 & 1 \end{bmatrix}$$

$$G = \begin{bmatrix} G_1 & 0 \\ 0 & G_2 \end{bmatrix}, N = \begin{bmatrix} N_1 & 0 \\ 0 & N_2 \end{bmatrix} = \begin{bmatrix} f_1(x_1) & 0 \\ 0 & f_2(x_2) \end{bmatrix}$$

$$X = \begin{bmatrix} x_1 \\ x_2 \end{bmatrix} = AX = -HGN$$

$$X = \begin{bmatrix} -G_1 & -G_2 \\ G_1 & -G_2 \end{bmatrix} \begin{bmatrix} f_1(x_1) & 0 \\ 0 & f_2(x_2) \end{bmatrix} \begin{bmatrix} x_1 \\ x_2 \end{bmatrix}$$

$$\text{Or } X = \begin{bmatrix} x_1 \\ x_2 \end{bmatrix} = \begin{bmatrix} -G_1 f_1(x_1) & -G_2 f_2(x_2) \\ G_1 f_1(x_1) & -G_2 f_2(x_2) \end{bmatrix}$$

$$\begin{bmatrix} x_1 \\ x_2 \end{bmatrix} = \begin{bmatrix} -G_1 f_1(x_1)x_1 & -G_2 f_2(x_2)x_2 \\ G_1 f_1(x_1)x_1 & -G_2 f_2(x_2)x_2 \end{bmatrix}$$

Or $x_1 = (-x_1 G_1 f_1(x_1) - x_2 G_2 f_2(x_2))$ and

$$x_2 = x_1 G_1 f_1(x_1) - x_2 G_2 f_2(x_2)$$

With state feedback gain matrix $K = [k_1 \ k_2]$, $B = \begin{bmatrix} 0 \\ 1 \end{bmatrix}$

$$BK = \begin{bmatrix} 0 \\ 1 \end{bmatrix} [k_1 \ k_2] = \begin{bmatrix} 0 & 0 \\ k_1 & k_2 \end{bmatrix}$$

From Fig. 9, $A_b = (A - BK)$.

$$\text{Hence } X_b = \begin{bmatrix} X_{1b} \\ X_{2b} \end{bmatrix} = A_b X_b = (A - BK) X_b$$

$$\text{Hence } A_b = \left\{ \begin{bmatrix} -G_1 f_1(x_1) & -G_2 f_2(x_2) \\ G_1 f_1(x_1) & -G_2 f_2(x_2) \end{bmatrix} - \begin{bmatrix} 0 & 0 \\ k_1 & k_2 \end{bmatrix} \right\}$$

$$\text{Hence } X_b = \begin{bmatrix} X_{1b} \\ X_{2b} \end{bmatrix} = A_b X$$

$$= \left\{ \begin{bmatrix} -G_1 f_1(x_1) & -G_2 f_2(x_2) \\ G_1 f_1(x_1) & -G_2 f_2(x_2) \end{bmatrix} - \begin{bmatrix} 0 & 0 \\ k_1 & k_2 \end{bmatrix} \right\} \begin{bmatrix} x_1 \\ x_2 \end{bmatrix}$$

$$= \left\{ \begin{bmatrix} -G_1 f_1(x_1) - 0 & -G_2 f_2(x_2) - 0 \\ G_1 f_1(x_1) - k_1 & -G_2 f_2(x_2) - k_2 \end{bmatrix} \right\} \begin{bmatrix} x_1 \\ x_2 \end{bmatrix}$$

$$= \begin{bmatrix} -G_1 f_1(x_1)x_1 - G_2 f_2(x_2)x_2 \\ (G_1 f_1(x_1) - k_1)x_1 - (G_2 f_2(x_2) - k_2)x_2 \end{bmatrix}$$

$$\text{Hence } X_{1b} = -x_1 G_1 f_1(x_1) - x_2 G_2 f_2(x_2)$$

$$X_{2b} = x_1(G_1 f_1(x_1) - k_1) - x_2(G_2 f_2(x_2) - k_2)$$

From above two equations:

$$X_{1b} = -G_1 Y_1 - G_2 Y_2 = -C_1 - C_2 \quad (34a)$$

$$\begin{aligned} X_{2b} &= G_1 Y_1 - x_1 k_1 - G_2 Y_2 + x_2 k_2 \\ &= C_1 - C_2 - x_1 k_1 + x_2 k_2 \quad (34b) \end{aligned}$$

Eq. (34a) and Eq. (34b) are additionally used for digital simulation with state feedback in conjunction with the digital simulation used in section 3.2.

4 Conclusion

The governing equation under limit cycling condition (autonomous system i.e. $u = 0$) in frequency response form is $X = -HC$ and $C = GN(X)$; leading to $X = -HGN(X)$ $X = AX$, where $A = -HGN(x)$: which facilitates the determination of Eigen values of the general multivariable systems.

The governing equation with **state feedback** is $\frac{d}{dt}[x(t)] = (A - BK) X$: which facilitates the determination of feedback gain matrix K for closed loop poles / Eigen values placement where the limit cycles are suppressed / eliminated in the general multivariable systems.

The present work claims the novelty in the following respects. The Poles / Eigen values are determined for Limit Cycling Systems with Memory type nonlinearities or the nonlinearities whose describing functions (harmonic linearization) are complex functions of X and

ω . It would be extremely difficult to formulate and simplify the expressions in the harmonic balance method [10]. It is felt necessary to develop a graphical technique using harmonic balance method as discussed in the reference [11]. The poles of such systems are shifted or placed suitably by **state feedback** so that the systems do not exhibit limit cycles. The pole placement is done either arbitrary selection satisfying the state controllability condition or by optimal selection of feedback gains Matrix K using Riccati Equation. The optimal selection of feedback gain matrix K has not been address elsewhere.

There is an ample scope of extension of the present work for prediction of limit cycles and its suppression in 3×3 memory type nonlinear systems, which may subsequently have extended for $n \times n$ memory type nonlinear multivariable systems. This work may be taken up in future in conjunction with the procedure stated in reference [9] for prediction of limit cycles in 3×3 non-memory type nonlinear systems [3], [9].

Acknowledgement:

The Authors wish to thank the C.V Raman Global University, Bhubaneswar – 752054, Odisha, India for providing the computer facilities for carrying out the research and preparation of this paper.

References:

- [1] A. Chidambaram and S. Velusami, Decentralized biased controllers for load-frequency control of inter connected power systems considering governor dead band non-linearity, *INDICON*, 2005, Annual IEEE, pp.521-525.
- [2] K.C Patra and Y.P Singh, Structural formulation and prediction of limit cycle for multivariable nonlinear systems, *IETE Tech. Rev.*, vol. 40, 1994, pp. 253-260.
- [3] K. C Patra and A. Patnaik, Possibility of Quenching of Limit Cycles in Multi Variable Nonlinear Systems with Special attention to 3X3 Systems, *WSEAS Transactions on systems and control*, vol.18, 2023.
- [4] T.S. Tsay, Load Frequency control of interconnected power system with governor backlash nonlinearities, *Electrical Power and Energy*, vol. 33, 2011, pp.1542-1549.
- [5] C. Wang, M. Yang, W. Zheng, K. Hu, and D. Xu, Analysis and suppression of limit cycle oscillation for Transmission System with backlash Nonlinearity, *IEEE Transactions on Industrial Electronics*, vol. 62, (12), 2017, pp. 9261-9270,.
- [6] Z. Shi and Z. Zuo, Back stepping control for gear transmission servo systems with backlash nonlinearity, *IEEE Trans. Autom. Sci. Eng.*, vol. 12, (2), 2015, pp.752-757.
- [7] K. Ogata, *Modern Control Engineering*, 5th edition, PHI Learning, 2012.
- [8] Raymond T. Stefani, B. Shahian, Clement J. Savant, Jr., G. H. Hostetter, *Design of Feedback Control Systems*, 4th edition, Oxford University Press, 2002.
- [9] K. C Patra and A. Patnaik, Investigation of the Existence of Limit Cycles in Multi Variable Nonlinear Systems with Special Attention to 3x3 Systems, *Int. Journal of Applied Mathematics, Computational Science and System Engineering*. Vol. 5, 2023, pp. 93-114.
- [10] K.C. Patra, B. B. Pati and A. Lozowicki, Structural Formulation and Self-Oscillation Prediction in Multidimensional Nonlinear Closed-Loop Autonomous Systems, *Int. J. App. Math. And Comp. Sci.*, Vol 9, No. 2, 1999, pp 327-346,
- [11] K.C Patra and B.K Dakua, Investigation of limit cycles and signal stabilisation of two dimensional systems with memory type nonlinear elements, *Archives of Control Sciences*, vol. 28, (2), 2018, pp.285-330.
- [12] R. Genesio, A. Tesi, On limit cycles in feedback polynomial systems, *IEEE Trans. Circuits and Systems*, vol. 35, 1988, pp.1523-1528.
- [13] A. Gelb, Limit cycles in symmetric multiple nonlinear systems. *IEEE Trans. Autumn. Control: AC-8*, 1963, pp. 177-178.
- [14] H. Zak. Stanislaw, *Systems and Control*, Oxford University Press, 2003.
- [15] D. P. Atherton, *Nonlinear Control Engineering*, Van Nostrand Reinhold Company Limited, Molly Millar's Lane, Wokingham, Berks, 1975.
- [16] H.G. Jud, Limit cycle determination of parallel linear and non- linear elements. *IEEE Trans. Autumn. Control: AC-9*, 1964, pp. 183-184.
- [17] R. Gran, and M. Rimer, Stability analysis of systems with multiple nonlinearities. *IEEE Trans. Autumn. Control: 10*, 1965, pp. 94-97.
- [18] E.J. Davison, and D. Constantinescu, Describing function technique for multiple nonlinearity in a single feedback system *IEEE Trans Autumn. Control: AC-16*: 1971, pp. 50-60.
- [19] R. Oldenburger, T. Nakada, Signal stabilisation of self - oscillating system *IRE Trans. Automat Control. USA*, 6, 1961, pp: 319-325.
- [20] N. Viswandham and B.L. Deekshatulu, Stability analysis of nonlinear multivariable systems. *Int. J. Control*, 5, 1966, pp. 369-375.
- [21] A. Gelb and W.E. Vader-Velde, *Multiple-input describing functions and nonlinear system design*, McGraw- Hill, New York, 1968.
- [22] P.N. Nikiporuk, and B.L.M. Wintonyk, Frequency response analysis of two-dimensional nonlinear symmetrical and non-symmetrical control systems. *Int. J. Control*, 7, 1968, pp.49-62.
- [23] G.S. Raju, and R. Josselson, Stability of reactor control systems in coupled core reactors, *IEEE Trans. Nuclear Science*, NS-18, 1971, pp. 388-394.
- [24] D.P. Atherton, and, H.T.A. Dorrah survey on nonlinear oscillations, *Int. J. Control*, 31. (6), 1980, pp. 1041-1 105.
- [25] J. O. Gray and N.B. Nakhala, Prediction of limit cycles in multivariable nonlinear systems. *Proc. IEE, Part-D*, 128, 1981 pp. 233-241.
- [26] A.I. Mees, Describing function: Ten years on. *IMA J. Appl. Math.*, 34, 1984 pp. 221-233.

- [27] L. Sebastian, The self-oscillation determination to a category of nonlinear closed loop systems, *IEEE Trans. Autumn. Control*, AC-30, (7), 1985 pp. 700-704.
- [28] P.A. Cook, *Nonlinear dynamical systems*, Prentice-Hall, Englewood Cliffs, NJ, 1986.
- [29] H.C. Chang, C.T. Pan, C.L. Huang, and C.C. Wei, A general approach for constructing the limit cycle loci of multiple nonlinearity systems, *IEEE Trans. Autumn. Control*, AC-32, (9), 1987, pp. 845-848.
- [30] A.G. Parlos, A.F. Henry, F.C. Schweppe, L.A. Gould and D. D. Lanning, Nonlinear multi variable control of nuclear power plants based on the unknown but bounded disturbance model, *IEEE Trans. Autumn. Control*, AC-33, (2), 1988 pp. 130-134.
- [31] V.K. Pillai, and, H.D.Nelson, A new algorithm for limit cycle analysis of nonlinear systems, *Trans. ASME, J. Dyn. Syst. Meas. Control*, 110, 1988, pp. 272-277.
- [32] O.R Fendrich, Describing functions and limit cycles, *IEEE Trans. Autom. Control*, AC -31, (4), 1992, pp. 486487.
- [33] M. Zhuang and D. P. Huang, PID controller design for TITO system, *TEE Proc. Control Theory Appl.* 141, (2), 1994, pp. 111-120.
- [34] A. P. Loh and V.V. Vasanu, Necessary conditions for limit cycles in multi loop relay systems, *IEE Proc., Control Theory Appl.*, 141, 31, 1994, pp. 163-168.
- [35] A. Tesi, et al., Harmonic balance analysis of periodic doubling bifurcations with implications for control of nonlinear dynamics, *Automatic*, 32 (9), 1996, 1255, 1271.
- [36] C.H. Lin and K.W Han, Prediction of Limit cycle in Nonlinear two input two output control system, *IEE Proc.-Control Theory Appl.* Vol.146, No.3 May, 1999.
- [37] Y. Hori, et al., Slow resonance ratio control for vibration suppression and disturbance rejection in torsional system, *IEEE Trans. Ind. Electron.*, vol. 46, (1), 1999, pp.162-168.
- [38] M. Nordin and P. O. Gutman, Controlling mechanical systems with backlash- a survey, *Automatica*, vol. 38, (10), 2002, pp.1633-1649.
- [39] M. Eftekhari and S. D. Katebi, Evolutionary Search for Limit Cycle and Controller Design in Multivariable nonlinear systems, *Asian Journal of Control*, Vol. 8, No. 4, 2006, pp. 345 – 358.
- [40] M Katebi, et al., Limit Cycle Prediction Based on Evolutionary Multi objective Formulation, *Hindawi Publishing Corporation, Mathematical Problems in engineering* Volume, Article ID 816707, 2009, 17pgs.
- [41] J Garrido, et al., Centralized PID control by Decoupling of a Boiler-Turbine Unit, *Proceedings of the European Control Conference*, Budapest, Hungary, Aug. 2009, 23-26.
- [42] T.S. Tsay, Limit Cycle prediction of nonlinear multivariable feedback control systems with large transportation lags, *Hindawi Publishing corporation journal of control science and Engineering*, Vol., article ID 169848, 2011.
- [43] T.S. Tsay, Stability Analysis of Nonlinear Multivariable Feedback Control systems, *WSEAS Transactions on systems*, Volume 11, Issue 4, 2012, pp. 140 – 151.
- [44] V. Sujatha, R. C. Panda, Relay Feedback Based Time domain modelling of Linear 3-by-3 MIMO System, *American Journal of System Science*, Scientific & Academic Publishing, 1(2) 2012, pp. 17-22.
- [45] C. Wang, et al., Vibration suppression with shaft torque limitation using explicit MPC-PI switching control in elastic drive systems, *IEEE Trans. Ind. Electron*, vol. 62,(11), 2015, pp. 6855-6867.
- [46] M. Yang, et al., Suppression of mechanical resonance using torque disturbance observer for two inertia system with backlash *Proc. IEEE 9th Int. Conf. Power Electron.*, ECCE Asia, 2015, pp. 1860 - 1866.
- [47] D. S. Lopez and A.P Vega, Fuzzy Control of a Toroidal Thermosyphon for Known Heat Flux Heating Conditions, *Proceeding of the 8th World Congress on Momentum, Heat and Mass Transfer (MHMT'23)*, Lisbon Portugal-March 26-28, 2023. DOI:10.11159/enfht23.133.
- [48] C. Corrado, et. al, Quantifying the impact of shape uncertainty on predict arrhythmias, *Computers in Biology and Medicine, Elsevier Ltd.*, 153, 2023, 106528.
- [49] W. Chen., et. al, Oscillation characteristics and trajectory stability region analysis method of hierarchical control microgrids, *Energy Reports*, 9, 2023, pp 315-324.
- [50] U. Kumar, et.al., The effect of sub diffusion on the stability of autocatalytic systems, *Chemical Engineering Science, Elsevier Ltd.*, 265, 2023, 118230.
- [51] J. I Marrone, et.al., A nested bistable module within a negative feedback loop ensures different types of oscillations in signalling systems, *Scientific reports/ Nature portfolio*, 2023, 13:529.
- [52] S. B. Munch, et.al., Recent developments in empirical dynamic modelling, *Methods in Ecology and Evolution*, 2022, 14, pp 732-745.

Contribution of Individual Authors to the Creation of a Scientific Article (Ghostwriting Policy)

Kartik Chandra Patra has formulated the problem, methodology of analysis adopted and algorithm of computation presented.

Asutosh Patnaik has made the validation of the results using the geometric tools and SIMULINK toolbox of MATLAB software

Sources of Funding for Research Presented in a Scientific Article or Scientific Article Itself

The C.V. Raman Global University has provided all computer facilities with relevant software for the research work and also for the preparation of the paper

Conflict of Interest

The authors have no conflicts of interest to declare that are relevant to the content of this article

Creative Commons Attribution License 4.0 (Attribution 4.0 International, CC BY 4.0)

This article is published under the terms of the Creative Commons Attribution License 4.0

https://creativecommons.org/licenses/by/4.0/deed.en_US